Acta Crystallographica Section D
Biological Crystallography
ISSN 0907-4449

Structures of D-amino-acid amidase complexed with L-phenylalanine and with L-phenylalanine amide: insight into the D-stereospecificity of D-amino-acid amidase from *Ochrobactrum anthropi* SV3

Seiji Okazaki,[a] Atsuo Suzuki,[a] Tsunehiro Mizushima,[a] Hidenobu Komeda,[b] Yasuhisa Asano[b] and Takashi Yamane[a]*

[a]Department of Biotechnology, School of Engineering, Nagoya University, Chikusa, Nagoya 464-8603, Japan, and [b]Biotechnology Research Center, Toyama Prefectural University, Imizu, Toyama 939-0398, Japan

Correspondence e-mail: yamane@nubio.nagoya-u.ac.jp

Received 11 October 2007
Accepted 18 December 2007

PDB References: D-amino-acid amidase-L-phenylalanine complex, 2efu, r2efusf; D-amino-acid amidase-L-phenylalanine amide complex, 2efx, r2efxsf.

The crystal structures of D-amino-acid amidase (DAA) from *Ochrobactrum anthropi* SV3 in complex with L-phenylalanine and with L-phenylalanine amide were determined at 2.3 and 2.2 Å resolution, respectively. Comparison of the L-phenylalanine amide complex with the D-phenylalanine complex reveals that the D-stereospecificity of DAA might be achieved as a consequence of three structural factors: (i) the hydrophobic cavity in the region in which the hydrophobic side chain of the substrate is held, (ii) the spatial arrangement of Gln310 O and Glu114 $O^{\varepsilon 2}$ that fixes the amino N atom of the substrate and (iii) the existence of two cavities that keep the carboxyl/amide group of the substrate near or apart from Ser60 O^{γ}.

1. Introduction

D-Amino-acid amidase (DAA) from the soil bacterium *Ochrobactrum anthropi* SV3, composed of 363 amino-acid residues, catalyzes the D-stereospecific hydrolysis of amino-acid amides with bulky hydrophobic side chains to yield D-amino acids and ammonia (Fig. 1*a*; Asano *et al.*, 1989; Komeda & Asano, 2000). Recently, a new method that combines an amino-acid amide racemase with a D-stereospecific hydrolase such as DAA was developed. This method can be used to produce D-amino acids with a theoretical yield of 100% (Asano & Yamaguchi, 2005*a*,*b*). This method requires D-stereospecific hydrolases with a high D-stereospecificity in order to achieve the greatest theoretical yield of product.

We have previously reported the crystal structures of DAA in the native form and in a complex with D-phenylalanine (D-Phe) at 2.1 and 2.4 Å resolution, respectively (Okazaki *et al.*, 2007). DAA contains a Ω-loop (residues 207–223) at the entrance to the active site like other penicillin-recognizing proteins (Davies *et al.*, 2001; Nukaga *et al.*, 2004). Interestingly, a pseudo-acyl intermediate was found in the D-Phe-containing complex. By comparing the structures, we were able to identify the substrate-recognition residues of DAA (Okazaki *et al.*, 2007). However, these structures did not address why DAA does not exert activity on L-amino-acid amides. Understanding the specific substrate-recognition mechanism of DAA is important for more general understanding of D,L-stereospecificity and has the potential to lead to the improved design of engineered enzymes useful for industrial applications.

In this study, the crystal structures of DAA in complex with L-phenylalanine (L-Phe) and with L-phenylalanine amide (L-Phe-NH_2) were determined at 2.3 and 2.2 Å resolution, respectively.

2. Materials and methods

2.1. Preparation of L-Phe and L-Phe-NH_2 complexes

DAA was purified as described previously (Komeda & Asano, 2000). The crystallization conditions of native DAA were as described elsewhere (Okazaki *et al.*, 2007). Plate-shaped crystals grew to dimensions of 0.5 × 0.05 × 0.03 mm within 10 d. The complexes were prepared by soaking DAA crystals in a solution containing the

Table 1
Data-collection and refinement statistics.

Values in parentheses are for the highest resolution shell.

	L-Phe complex	L-Phe-NH_2 complex
Data collection		
Space group	$P2_1$	$P2_1$
Unit-cell parameters		
a (Å)	77.5	76.7
b (Å)	123.3	123.4
c (Å)	116.2	115.5
β (°)	104.0	104.4
Wavelength (Å)	1.0	1.0
Resolution (Å)	50–2.3 (2.38–2.30)	50–2.2 (2.28–2.20)
R_{merge}† (%)	9.3 (35.9)	7.2 (26.5)
Average $I/\sigma(I)$	17.0 (3.6)	14.6 (2.3)
Completeness (%)	100 (100)	98.1 (85.6)
Multiplicity	6.1 (6.0)	4.7 (3.1)
Refinement		
Resolution (Å)	47.7–2.3	19.8–2.2
No. of unique reflections	89171	97895
R_{work}/R_{free}	0.171/0.235	0.187/0.256
No. of non-H atoms		
Protein	16410	16144
Ligand	72	72
Barium ions	26	22
Water molecules	1407	1188
R.m.s. deviations		
Bond lengths (Å)	0.010	0.012
Bond angles (°)	1.26	1.35
Ramachandran plot		
Allowed region (%)	91.3	90.4
Additionally allowed region (%)	8.3	8.9
Generously allowed region (%)	0.5	0.7
Disallowed regions (%)	0.0	0.0

† $R_{merge} = \sum_{hkl}\sum_i |I_i(hkl) - \langle I(hkl)\rangle| / \sum_{hkl}\sum_i I_i(hkl)$, where $I_i(hkl)$ is the observed intensity and $\langle I(hkl)\rangle$ is the mean intensity.

product or substrate enantiomer (L-Phe or L-Phe-NH_2). DAA crystals were soaked in a solution (27% PEG 3350, 0.06 *M* barium chloride and 0.1 *M* MES pH 6.9) containing 20 m*M* enantiomer. The soaking time for L-Phe or L-Phe-NH_2 was 12 or 2.5 h, respectively. Crystals were then moved into a cryogenic solution (30% PEG 3350, 0.06 *M* barium chloride and 0.1 *M* MES pH 6.9) containing 20 m*M* enantiomer and soaked for a few seconds.

2.2. Data collection, structure determination and refinement

X-ray data for the L-Phe complex were collected to 2.3 Å resolution at 100 K at the BL38B1 station, SPring-8, Hyogo, Japan. X-ray data for the L-Phe-NH_2 complex were collected to 2.2 Å resolution at 100 K at the BL41XU station, SPring-8. These data were processed using *HKL*-2000 (Otwinowski & Minor, 1997) and the *CCP*4 program suite (Collaborative Computational Project, Number 4, 1994).

The initial phase set used to solve the structures of the L-Phe and L-Phe-NH_2 complexes was calculated from the structure of native DAA (PDB code 2drw). Crystallographic refinement was carried out using the program *REFMAC*5 (Murshudov *et al.*, 1997) from the *CCP*4 program suite (Collaborative Computational Project, Number 4, 1994) and manual model rebuilding was performed using the graphics program *Coot* (Emsley & Cowtan, 2004). Enantiomers were located at the active sites using a σ_A-weighted $F_o - F_c$ OMIT map (Read, 1986). Water molecules were added using the program *ARP*/*wARP* v.6.0 (Perrakis *et al.*, 1999). The number of intermolecular contacts within 4.1 Å was calculated using *NCONT* from the *CCP*4 program suite (Collaborative Computational Project, Number 4, 1994). The data-collection and refinement statistics are summarized in Table 1. *CCP*4*MG* (Potterton *et al.*, 2004) was used to produce all of the figures presented with the exception of Figs. 1(*a*) and 2(*d*).

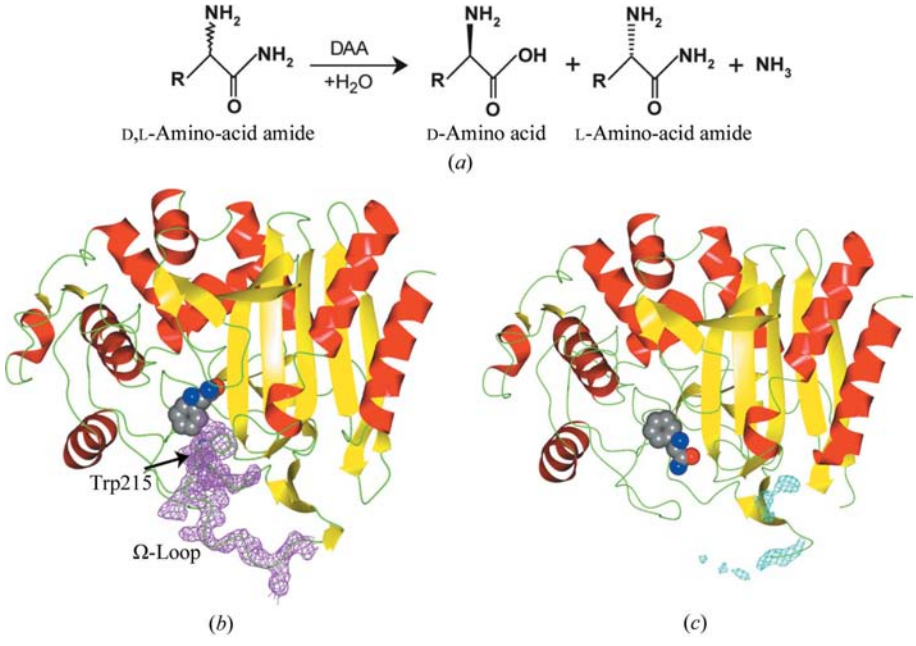

Figure 1
(*a*) Stereoselective reaction of DAA. (*b*) Overall structure of molecule *A* (ordered type) in the complex with L-Phe-NH_2. α-Helices are shown as red ribbons and β-strands are shown as yellow arrows. L-Phe-NH_2 is represented by spheres; C atoms are grey, O atoms red and N atoms blue. A $2F_o - F_c$ density map (1σ level; in magenta) is superimposed on the Ω-loop (residues 210–223). Trp215 is represented by a cylinder model. (*c*) Overall structure of molecule *E* (disordered type) in the complex with L-Phe-NH_2. A σ_A-weighted $F_o - F_c$ OMIT map (residues 205, 206, 223 and 224) contoured at 3.0σ is superposed in cyan.

3. Results and discussion

3.1. Ordered and disordered conformation observed in the Ω-loop

The overall structure of the L-Phe complex is essentially the same as that of the L-Phe-NH_2 complex. The enantiomers were located at the active sites of each of the six molecules in the asymmetric unit. In the L-Phe-NH_2 complex, the average *B* factors of the main-chain atoms for molecules *A*, *B*, *C*, *D*, *E* and *F* are 28.4, 30.9, 24.5, 23.0, 36.9 and 58.6 $Å^2$, respectively. The average *B* factor of each enantiomer is almost equal to that of its bound molecule.

In the L-Phe and L-Phe-NH_2 complexes, the molecules in the asymmetric unit can be classified into two types from the visibility of the electron density of the Ω-loop: an ordered type (molecules *A*, *B* and *C*) with clear electron density for the Ω-loop and a disordered type (molecules *D*, *E* and *F*) with poor electron density in the Ω-loop region.

The location of the enantiomers differs in a way that correlates with

DAA taking on an ordered or disordered conformation. The carboxyl group of L-Phe and the amide group of L-Phe-NH_2 point towards the nucleophilic Ser60 O^{η} of DAA when the Ω-loop is ordered (molecules *A*, *B* and *C*; Fig. 1*b*). In contrast, the carboxyl group of L-Phe and the amide group of L-Phe-NH_2 point towards the exterior side when the Ω-loop is disordered (molecules *D*, *E* and *F*; Fig. 1*c*).

The ordered or disordered conformations of the Ω-loops seem to be governed by the crystal-packing contacts around them. The crystal-packing contacts for the Ω-loop (residues 207–223) in each molecule showed that the crystal-packing contacts for the Ω-loop in molecule *E* were smaller than those for molecule *A*. Therefore, we supposed that the structure of molecule *E* is more similar to that in solution than that of molecule *A*.

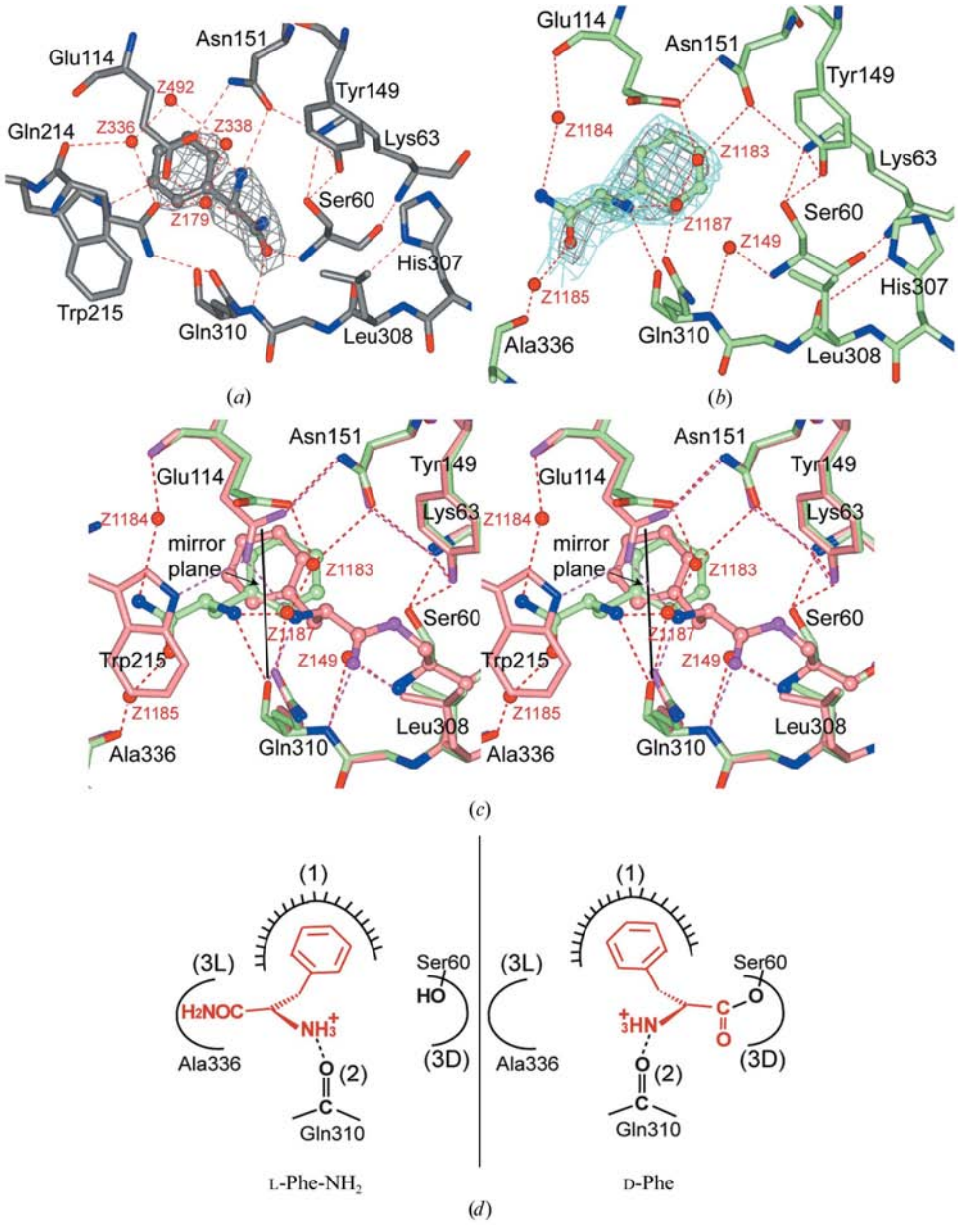

Figure 2
(*a*) Active-site residues of molecule *A* (ordered type) of the L-Phe-NH_2 complex. C atoms are shown in grey, O atoms in red and N atoms in blue. A σ_A-weighted $F_o - F_c$ L-Phe-NH_2 OMIT map contoured at 3.0σ is superposed in grey. Broken red lines represent hydrogen bonds. (*b*) Active-site residues of moleucle *E* (disordered type) of the L-Phe-NH_2 complex. C atoms are shown in light green. σ_A-Weighted $F_o - F_c$ L-Phe-NH_2 OMIT maps contoured at 3.0σ and 2.0σ are superposed in grey and cyan, respectively. (*c*) Stereoview of the superposition of the active-site residues of molecule *E* in the L-Phe-NH_2 complex and those in the D-Phe complex. The hypothetical mirror plane is shown as a black line. For the L-Phe-NH_2 complex, C atoms are shown in light green and hydrogen bonds are shown as red broken lines. For the D-Phe complex, C atoms are shown in pink and hydrogen bonds are shown as magenta broken lines. (*d*) Schematic representation of the binding mode of L-Phe-NH_2 and D-Phe in molecule *E* of DAA. L-Phe-NH_2 and D-Phe are shown in red. The hydrophobic cavity for holding the side chain and the space for anchoring the amino N atom are labelled (1) and (2), respectively. The cavities in which the amide group of L-Phe-NH_2 and the carboxyl group of D-Phe are located are labelled (3L) and (3D), respectively.

In the ordered-type structure (of which molecule *A* is a representative), the orientations of the enantiomers are similar to those observed for D-Phe in the D-Phe complex (Okazaki *et al.*, 2007). The formation of a covalent bond between Ser60 O^{γ} and the carbonyl C atom of the enantiomer does not occur in either complex (Fig. 2*a*), whereas formation of a covalent bond was observed in the D-Phe complex.

In the disordered-type structure (of which molecule *E* is a representative), the phenyl ring of the enantiomer makes use of the hydrophobic cavity as in the ordered type. However, the carboxyl group of L-Phe and the amide group of L-Phe-NH_2 are directed towards the exterior cavity that is occupied by the side chain of Trp215 from the Ω-loop in the ordered-type structure (Fig. 2*b*). In the disordered-type structure, this cavity is made by the hydrophobic side chains of Met119, Phe234 and Pro312, although the carboxyl or amide groups of the enantiomers are located in this area. Moreover, a water molecule is found at the oxyanion hole in the disordered-type structure.

3.2. Insight into the D-stereospecificity of DAA

The orientations of L-Phe-NH_2 and D-Phe are quite different in the disordered-type structures, although their phenyl rings are positioned in the highly hydrophobic cavity in both structures. The C^{α} atom of L-Phe-NH_2 is located in the region of the highly hydrophobic cavity, whereas Trp215 $N^{\varepsilon 1}$ from the Ω-loop is found in the cavity in the ordered-type structure. Both structures are roughly related to each other by hypothetical mirror symmetry, as shown in Fig. 2(*c*).

Comparison of molecule *E* in the L-Phe-NH_2 complex with that in the D-Phe complex presents three unique structural features that concern the difference in binding mode between L-Phe-NH_2 and D-Phe (Fig. 2*d*). The

first feature is the region of the hydrophobic cavity in which the aromatic ring of the substrate is held. The second feature is the spatial arrangement adopted by Gln310 O and the flexible side chain of Glu114, which is concerned with the anchoring of the amino N atom of L-Phe-NH_2 or D-Phe. The third is the existence of two cavities, one near Ser60 O^{γ} and another distant from Ser60 O^{γ}, which are occupied by the acylated carboxy group of D-Phe and the amide group of L-Phe-NH_2, respectively.

If the positions of the amino N atom and side chain are fixed, the position of the carboxyl group of the amino acid is uniquely located according to its chirality, *i.e.* L-amino acid or D-amino acid. The first two features of DAA, the hydrophobic cavity and the spatial arrangement taken on by Gln310 O and Glu114 $O^{\varepsilon 2}$, seem to be concerned with the positioning of the side chain and amino N atom of D-Phe and L-Phe-NH_2, respectively. The remaining carboxyl/amide group of D-Phe or L-Phe-NH_2 can then occupy either of the cavities mentioned as the third feature. As a consequence, the carboxyl group of D-Phe is uniquely located in the cavity near Ser60 O^{γ} and the amide group of L-Phe-NH_2 is uniquely located in another cavity distant from Ser60 O^{γ} (Fig. 2*d*). Therefore, the three features of DAA produce an environment in which only the carboxyl group of D-Phe can locate near the nucleophile Ser60 O^{γ}, leading to the high D-stereospecificity of DAA.

This work was supported in part by a research grant from the National Project on Protein Structural and Functional Analysis from the Ministry of Education, Culture, Sports, Science and Technology of Japan. The synchrotron-radiation experiments were performed at SPring-8 with the approval of the Japan Synchrotron Radiation Research Institute (JASRI; Proposal Nos. 2005B1793 and 2005B0372). We would like to thank Dr Shigenori Yamaguchi of Toyama Prefectural University for his help in the purification of DAA.

References

Asano, Y., Mori, T., Hanamoto, S., Kato, Y. & Nakazawa, A. (1989). *Biochem. Biophys. Res. Commun.* **162**, 470–474.
Asano, Y. & Yamaguchi, S. (2005*a*). *J. Mol. Catal. Ser. B*, **36**, 22–29.
Asano, Y. & Yamaguchi, S. (2005*b*). *J. Am. Chem. Soc.* **127**, 7696–7697.
Collaborative Computational Project, Number 4 (1994). *Acta Cryst.* D**50**, 760–763.
Davies, C., White, S. W. & Nicholas, R. A. (2001). *J. Biol. Chem.* **276**, 616–623.
Emsley, P. & Cowtan, K. (2004). *Acta Cryst.* D**60**, 2126–2132.
Komeda, H. & Asano, Y. (2000). *Eur. J. Biochem.* **267**, 2028–2035.
Murshudov, G. N., Vagin, A. A. & Dodson, E. J. (1997). *Acta Cryst.* D**53**, 240–255.
Nukaga, M., Kumar, S., Nukaga, K., Pratt, R. F. & Knox, J. R. (2004). *J. Biol. Chem.* **279**, 9344–9352.
Okazaki, S., Suzuki, A., Komeda, H., Yamaguchi, S., Asano, Y. & Yamane, T. (2007). *J. Mol. Biol.* **368**, 79–91.
Otwinowski, Z. & Minor, W. (1997). *Methods Enzymol.* **276**, 307–326.
Perrakis, A., Morris, R. & Lamzin, V. S. (1999). *Nature Struct. Biol.* **6**, 458–463.
Potterton, L., McNicholas, S., Krissinel, E., Gruber, J., Cowtan, K., Emsley, P., Murshudov, G. N., Cohen, S., Perrakis, A. & Noble, M. (2004). *Acta Cryst.* D**60**, 2288–2294.
Read, R. J. (1986). *Acta Cryst.* A**42**, 140–149.